

Chimia 54 (2000) 89–95  
 © Neue Schweizerische Chemische Gesellschaft  
 ISSN 0009–4293

# High-Resolution Spectroscopy of High Rydberg States

## Chemical and Technological Applications

Frédéric Merkt\*  
 Werner Prize Winner 1999

**Abstract:** High Rydberg states of atoms and molecules possess unusual properties that can be exploited in chemistry and technology. The extreme sensitivity of these states to external influences makes them ideal probes of their environment and they can be used to measure electric fields and ion concentrations in the gas phase with high accuracy. The highest Rydberg states with principal quantum number  $n \geq 200$  lie energetically so close to successive ionization thresholds in atoms and molecules that they can be used to determine ionization potentials precisely and to extract detailed information on the energy level structure of molecular cations. To investigate and better exploit the properties of high Rydberg states, we have developed new high-resolution vacuum ultraviolet laser sources and combined these with millimetre waves in double-resonance experiments. In these experiments a spectral resolution of up to 60 kHz can be achieved. High-resolution spectroscopy is ideally suited to study the fascinating behaviour of high Rydberg states and opens the way to promising applications in the gas-phase chemistry of unstable and charged particles and in measurement technology.

**Keywords:** High-resolution spectroscopy · Ionization potentials · Millimetre waves · Molecular Rydberg states · Photoelectron spectroscopy · Vacuum ultraviolet lasers



Frédéric Merkt was born on July 12, 1966 in Neuchâtel, Switzerland. He received his diploma in chemistry in 1988 from the ETH Zürich with Prof. Martin Quack as diploma thesis advisor. He obtained his Ph.D. in 1992 from the Uni-

versity of Cambridge for work carried out in the group of Dr. Tim Softley on the generation and spectroscopic applications of coherent extreme ultraviolet radiation. He then worked as a post-doctoral researcher at the University of Paris-Sud, Orsay (1992) with Dr. Paul Marie Guyon on the use of synchrotron radiation in the study of ion–molecule reactions and at Stanford University (1994) with Prof. Richard N. Zare on experimental investigations of the  $H + H_2$  reaction system. Before returning to the ETH Zürich as an assistant professor in 1995, he worked at Oxford University where he held a junior research fellowship at St. John's College (1992–1995). In 1999 he was elected full professor of physical chemistry at ETH Zürich. His research is devoted to the development of narrow bandwidth laser sources in the vacuum ultraviolet and their use in high-resolution photoionization and photoelectron spectroscopy and in the study of molecular Rydberg states. In 1999 he was awarded the Swiss National Latsis Prize. Frédéric Merkt is married and the father of four children.

### 1. High Rydberg States and Their Properties

Over the past four years my research group has followed a research program devoted to fundamental investigations of high atomic and molecular Rydberg states using high-resolution spectroscopy.

Rydberg states of atoms and molecules are electronically excited states, the energetic position of which can be described by Rydberg's formula [1]

$$E_n = E_{n=\infty} - hcR/(n-\delta_l)^2 \quad (1)$$

In Equation (1)  $h$ ,  $c$  and  $R$  are Planck's constant, the speed of light and Rydberg's constant, respectively.  $n$  represents the principal quantum number ( $n = 1, 2, \dots$ ) and  $\delta_l$  the quantum defect which depends on the orbital angular momentum quantum number  $l$  ( $l = 0, 1, \dots, n-1$ ). The states characterized by Equation (1) form an infinite series, a Rydberg series, which converges at  $n = \infty$  to the ionization limit.

Although atomic and molecular Rydberg states have been the object of scientific investigations for more than a century [1–7], the development of new spectroscopic techniques which exploit the prop-

erties of very high Rydberg states (with  $n \geq 100$ ), such as pulsed-field-ionization zero-kinetic-energy (PFI-ZEKE) photoelectron spectroscopy [8] and mass-analyzed threshold ionization (MATI) spectroscopy [9], has stimulated a new interest for the properties of high molecular Rydberg states (recent reviews are Refs. [10–14]) and provided our initial motivation.

Most physical and chemical properties of Rydberg states scale as integer powers of  $n$  and therefore vary rapidly with  $n$  [12]. An overview of the  $n$  dependence of selected properties is given in Table 1 which also contains representative numerical values. For instance, the binding energy of the Rydberg electron scales as  $n^{-2}$ , the size of the Rydberg electron orbital (roughly given by the radius of the Bohr orbit) as  $n^2$

\*Correspondence: Prof. Dr. F. Merkt  
 Laboratorium für Physikalische Chemie  
 ETH Zentrum  
 CH-8092 Zürich  
 Tel.: +41 1 632 43 67  
 Fax: +41 1 632 10 21  
 E-Mail: merkt@mw.phys.chem.ethz.ch

and the spacing between adjacent members of a Rydberg series as  $n^{-3}$ . The period of the electron orbiting motion which, in a classical picture, gives the time interval separating successive encounters of the Rydberg electron with the ionic core scales as  $n^3$ , and so does the lifetime of molecular Rydberg states; indeed, the decay of molecular Rydberg states by nonradiative processes such as autoionization or predissociation necessitates an energy exchange between the ion core and the Rydberg electron which can only efficiently take place when the electron returns to the immediate vicinity of the core. The increase of the lifetimes with  $n$ , and the resulting narrowing of the natural linewidths, make high-resolution spectroscopy ideally suited to study the properties of high Rydberg states.

It is apparent from the scaling laws summarized in Table 1 that high Rydberg states possess very unusual properties. These properties make high Rydberg states fascinating to investigate experimentally in their own right; they are also unusual enough that they can be exploited in novel chemical and technological applications. For example, the polarizability  $\alpha$  of Rydberg states scales with  $n^7$ . An atom in an  $n = 100$  Rydberg state is  $10^{14}$  times more sensitive to electric fields than in its ground state and can therefore be used as a very sensitive local electric field sensor (see Section 3 below). The rapid decrease of the binding energy with increasing  $n$  value can be used to determine ionization potentials of atoms and molecules experimentally with high accuracy by extrapolation to  $n = \infty$  using Equation (1).

When an applied electric field becomes equal to, or greater than, the atomic or molecular field that binds the Rydberg electron to the positively charged ion core, field ionization takes place. The value of the threshold field for field ionization scales as  $n^{-4}$ . This scaling law turns out to be of

great practical significance for the detection of high Rydberg states: Electrons or ions released by pulsed field ionization of Rydberg states can be detected easily and with almost 100% efficiency. Moreover, all Rydberg states located above a chosen  $n$  value can be selectively ionized by applying a suitably small ionizing electric field. The field ionization of high Rydberg states can be exploited to obtain precise spectroscopic information on molecular ions with high sensitivity (see Section 4 below).

## 2. High-Resolution Spectroscopy of High Rydberg States

The study of high Rydberg states poses several experimental challenges:

1. The Rydberg spectrum of most small-sized molecules lies in the vacuum ultraviolet (VUV,  $\lambda \leq 200$  nm) region of the electromagnetic spectrum where no commercial tunable laser systems are available, or even in the extreme ultraviolet (XUV,  $\lambda \leq 105$  nm) where no material is known that still transmits radiation. To carry out spectroscopic measurements in these regions one must develop one's own laser sources, hold laser light source, sample and detectors in the same vacuum system and make extensive use of differential pumping.
2. The rapid increase of the spectral density of Rydberg states with  $n$  (see Table 1) renders a high experimental resolution imperative: To resolve adjacent Rydberg states at  $n = 1000$ , a resolution of at least  $2 \cdot 10^{-4} \text{ cm}^{-1}$  (ca. 6 MHz) is required, and this at wavenumbers of more than  $10^5 \text{ cm}^{-1}$  above the ground neutral state.
3. The extreme sensitivity of high Rydberg states to even small external perturbations can easily falsify high-reso-

lution spectroscopic measurements and require magnetic shielding and the development and implementation of reliable diagnostic tools for the determination and elimination of weak stray electric fields.

The most general and broadly applicable approach to study atomic and molecular Rydberg states spectroscopically relies on the direct single-photon excitation from the ground neutral state using VUV or XUV radiation sources. Early studies were carried out using the continuous emission spectrum of high pressure rare gas lamps in combination with large monochromators [15][16]. Nowadays, these sources have been almost completely replaced by synchrotron radiation sources which offer the advantages of higher spectral brightness and broader tunability. However, the need to monochromatize the broad-band synchrotron radiation still limits the resolution achievable by modern synchrotrons to approximately  $1 \text{ cm}^{-1}$  in the range 10–20 eV [17]. Laser sources based on nonlinear optical processes in gases offer distinct advantages for high-resolution VUV spectroscopy: These sources do not necessitate a large-scale infrastructure, are relatively inexpensive and can be constructed and operated by a single experimentalist. Moreover, bandwidths significantly narrower than  $1 \text{ cm}^{-1}$  can be achieved by nonlinear frequency upconversion of commercial nanosecond dye lasers. The first VUV/XUV laser sources became operational in the Eighties [18–20] and soon found application in VUV spectroscopy in the range 10–17 eV [21–24] and more recently up to 20 eV [25][26].

Fig. 1 shows a schematic view of one of our VUV laser systems. Tunable radiation with frequency  $\nu_{\text{VUV}}$  is generated by two-photon resonance-enhanced sum- or difference-frequency mixing  $\nu_{\text{VUV}} = 2\nu_1 \pm \nu_2$  of two tunable visible or UV Nd:YAG-pumped dye lasers of frequency  $\nu_1$  and  $\nu_2$  using pulsed rare gas beams as nonlinear media. The dye laser frequencies can be doubled or tripled in nonlinear crystals such as  $\beta$ -Barium Borate (BBO) crystals with an efficiency of ca. 20%. The frequency of the first laser is held fixed at the position of a two-photon resonance of the nonlinear gas so as to enhance the VUV generation efficiency. Tunability of the VUV radiation is achieved by scanning the frequency  $\nu_2$  of the second laser. By a suitable choice of two-photon resonances in xenon, krypton and argon, the complete energy range between 8 eV and 20 eV can be covered with pulse energies up to  $10^{10}$  photons per laser pulse at repetition rates of 10–25 Hz. Starting from commercial

Table 1. The properties of high Rydberg states and their dependence on the principal quantum number  $n$

Property	$n$ dependence	Numerical Values		
		$n = 1$	$n = 100$	$n = 1000$
Mean radius	$n^2$	53 pm	0.53 $\mu\text{m}$	53 $\mu\text{m}$
Binding energy/ $\text{cm}^{-1}$	$n^{-2}$	109667 <sup>a</sup>	10.9	0.1
Period of electronic motion	$n^3$	0.15 fs	0.15 ns	150 ns
Spacing between levels/ $\text{cm}^{-1}$	$n^{-3}$	ca. 80000	0.2	$2 \cdot 10^{-4}$
Polarizability <sup>b</sup> /(MHz $\text{cm}^2/\text{V}^2$ )	$n^7$	$0.2 \cdot 10^{-7}$	$0.2 \cdot 10^7$	$0.2 \cdot 10^{14}$
Threshold ionization field/(V/cm)	$n^{-4}$	$\geq 10^8$	3.3	$3.3 \cdot 10^{-4}$

<sup>a</sup>For the hydrogen atom. <sup>b</sup>Values extrapolated from the value of the Na  $n = 10d$  Rydberg state.

pulsed dye lasers, a VUV bandwidth of  $0.1 \text{ cm}^{-1}$  can be achieved [27]. Recently, we have been able to construct a single-mode VUV laser system tunable in the range from 8 to 17 eV with a  $0.008 \text{ cm}^{-1}$  bandwidth by pulsed amplification of single-mode cw ring lasers [28]. After the nonlinear frequency upconversion process, the generated VUV radiation is separated from the fundamental frequencies in a vacuum monochromator and redirected towards the experimental region where it crosses a pulsed supersonic beam of the molecules or atoms to be studied at right angle. Ions and electrons produced by photoionization or pulsed field ionization are extracted by a pulsed electric field and directed through a flight tube to a multichannel plate (MCP) detector.

The lower panel in Fig. 2 shows a spectrum of  $s$  ( $l=0$ ) and  $d$  ( $l=2$ ) Rydberg series of argon in the range  $n = 40$ – $75$  converging on the lowest ionization threshold (corresponding to the production of a ground state  $^2P_{3/2} \text{Ar}^+$  ion). The spectrum was measured at a resolution of  $0.1 \text{ cm}^{-1}$  by monitoring the field ionization induced by a  $800 \text{ V/cm}$  pulsed electric field as a function of the VUV wavenumber. The upper panel displays a spectrum of  $n = 55$ – $57$  Rydberg states of argon belonging to series converging on the second ionization threshold of argon ( $\text{Ar}^+ ^2P_{1/2}$ ) recorded at a resolution of  $0.008 \text{ cm}^{-1}$  using our single-mode VUV laser [28]. These states lie above the lowest ionization limit and decay rapidly by spin-orbit autoionization. The broad asymmetric resonances correspond to very short-lived  $d$  Rydberg states and the sharper resonances to longer-lived  $s$  Rydberg states. The pronounced asymmetric line shapes are characteristic of autoionizing resonances and contain detailed information on the decay dynamics of the Rydberg states [29][30].

VUV laser spectroscopy is well suited to obtain spectroscopic and dynamical information on Rydberg states up to approximately  $n = 100$ . However, intrinsic limitations imposed by the bandwidth of these sources and by Doppler broadening (the Doppler shifts are proportional to the excitation frequency and are significant in the VUV even when collimated gas beams expanding perpendicularly to the propagation direction of the VUV radiation are used; at a wavenumber of  $100\,000 \text{ cm}^{-1}$ , the Doppler broadening of spectral lines of a gas expanding at a speed of  $500 \text{ m/s}$  in a cone with opening angle of  $10^\circ$  amounts to approximately  $0.03 \text{ cm}^{-1}$ ) prevent the investigation of the highest Rydberg states and the observation of the finer details of the energy level structure.

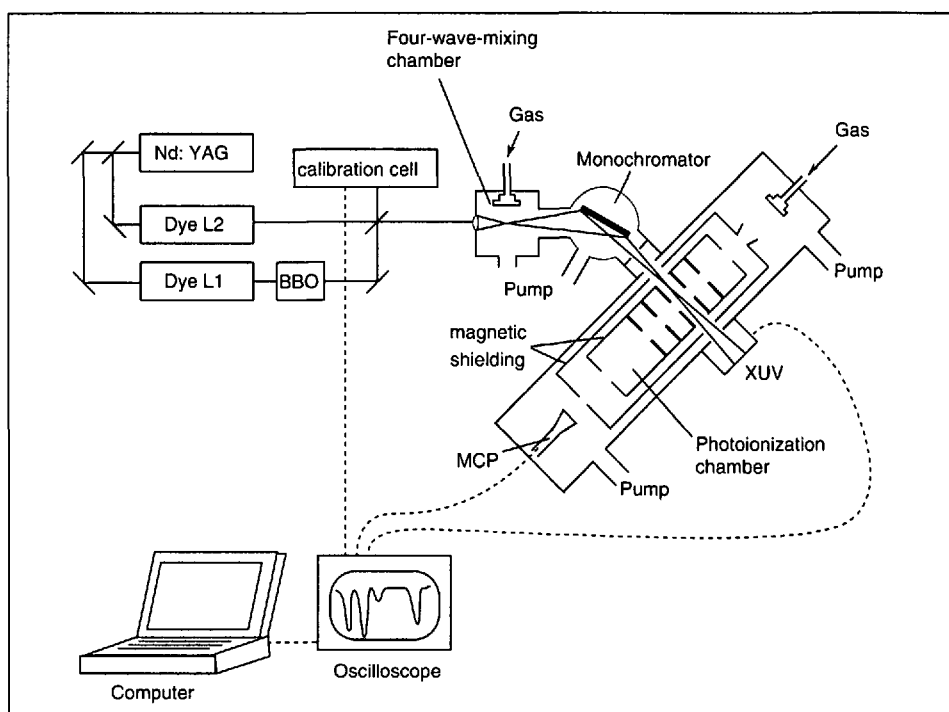


Fig. 1. Schematic view of a VUV laser system developed to study high Rydberg states.

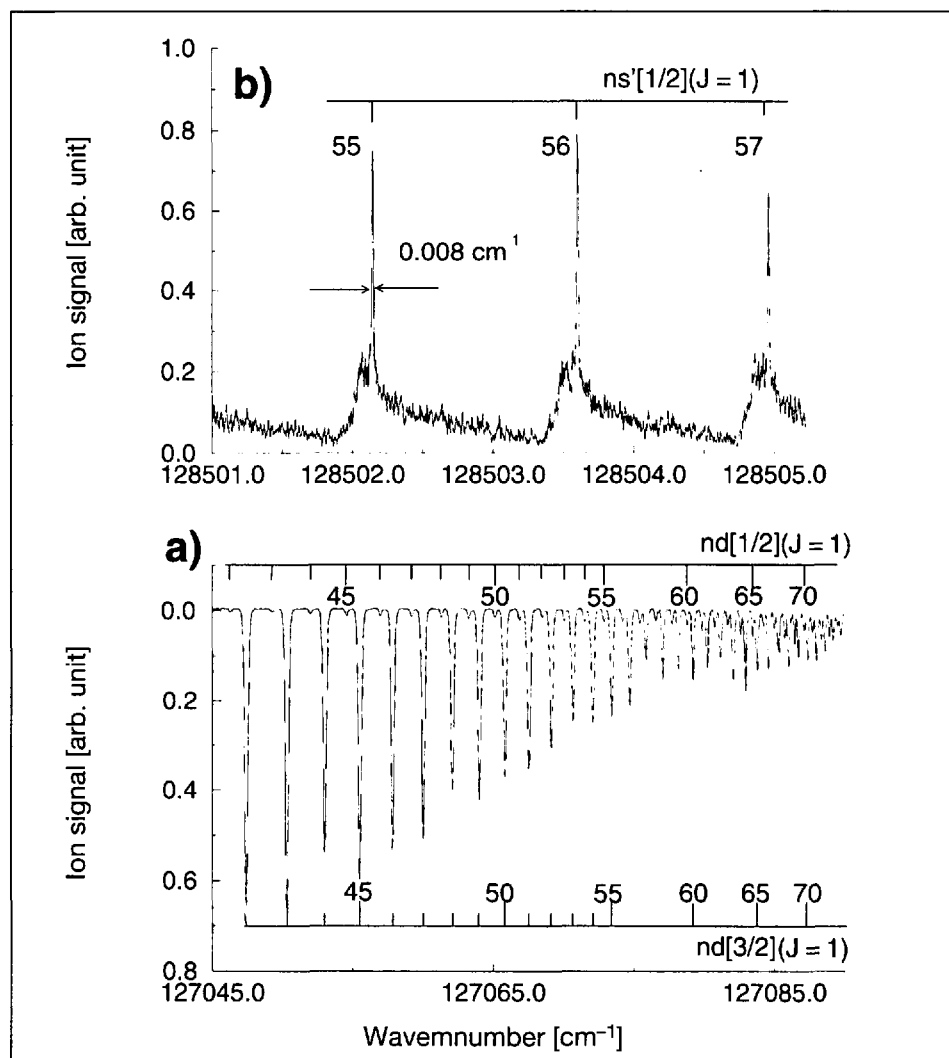


Fig. 2. High-resolution spectra of Rydberg states belonging to series converging on a) the lowest ( $\text{Ar}^+, ^2P_{3/2}$ ) and b) the first spin-orbit excited ( $\text{Ar}^+, ^2P_{1/2}$ ) ionization threshold of argon. The spectrum in a) was recorded at a resolution of  $0.1 \text{ cm}^{-1}$  using a broadly tunable VUV laser source and that in b) with a single-mode VUV laser enabling a resolution of  $0.008 \text{ cm}^{-1}$ . At a resolution of  $0.1 \text{ cm}^{-1}$ , the  $ns[3/2](J=1)$  series cannot be distinguished from the  $nd[3/2](J=1)$  series in trace a).

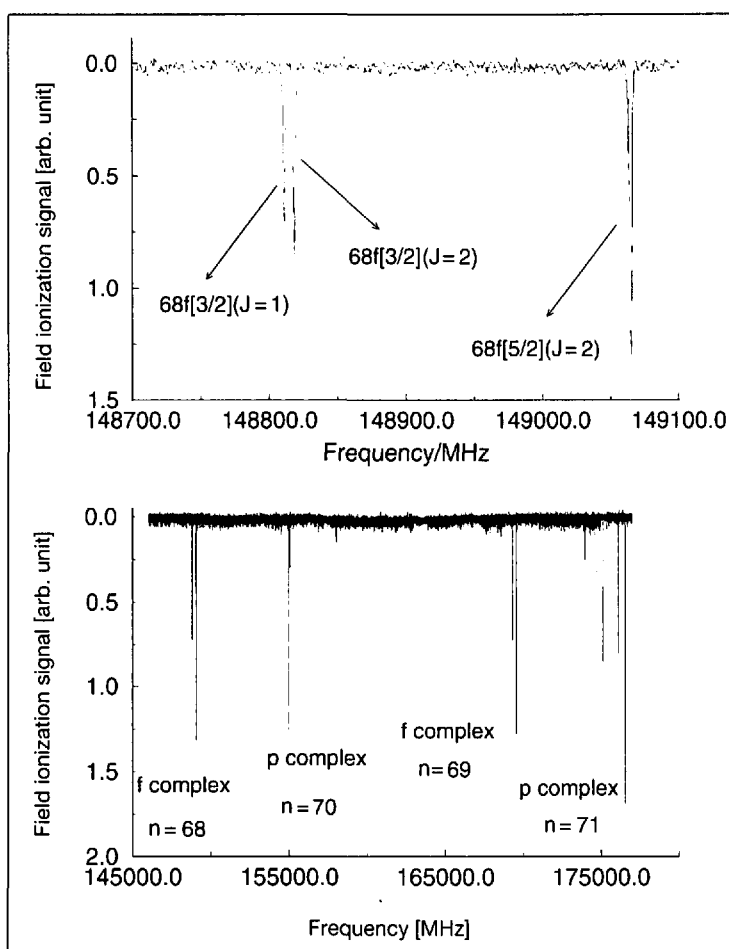


Fig. 3. Millimetre waves spectroscopy of Rydberg states of the argon atom. The lower panel shows a survey spectrum of transitions from the  $n = 62 d[3/2](J = 1)$  Rydberg state to  $p$  and  $f$  Rydberg states in the range  $n = 68-71$ . The upper panel shows an expanded view of the transition to the  $n = 68 f$  Rydberg state.

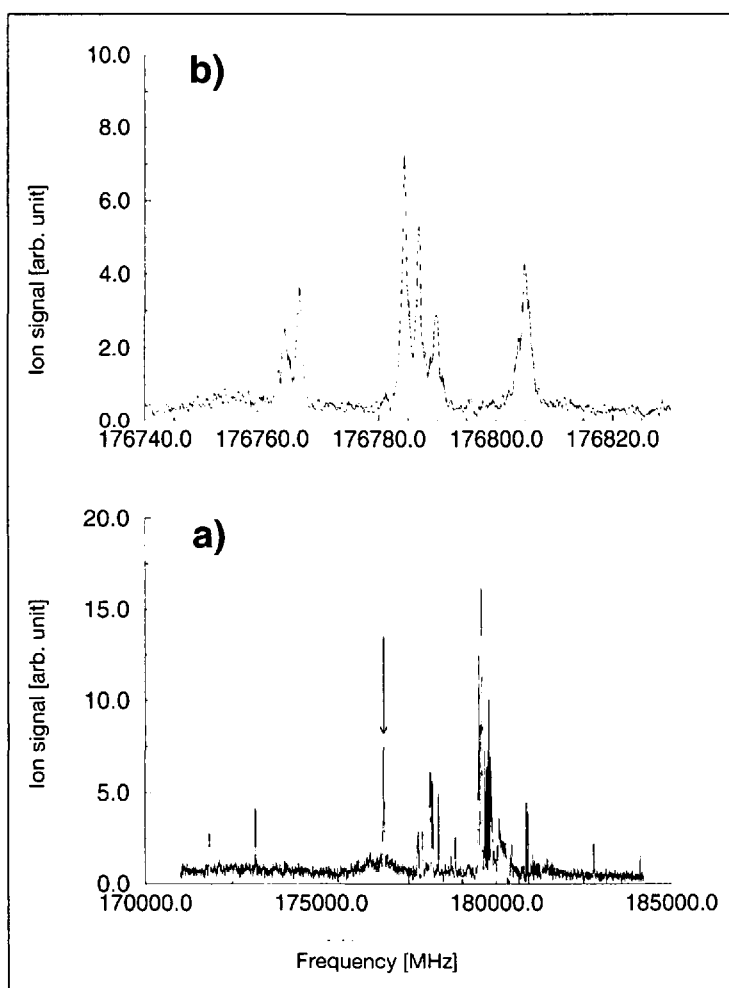


Fig. 4. Millimetre waves spectroscopy of high Rydberg states of the hydrogen molecule. The lower panel a) shows a survey spectrum of the transition between  $n = 51 d$  Rydberg states and  $n = 55 p$  and  $f$  Rydberg states belonging to series converging on the  $N^+ = 1$  rotational state of ortho- $H_2^+$ . A high-resolution spectrum of the line marked by an arrow in a) is displayed on an expanded scale in panel b).

To obtain such details, we use millimetre waves tunable in the range 120–180 GHz ( $4-6 \text{ cm}^{-1}$ ) in combination with VUV radiation in double-resonance experiments [31]. In these experiments, the frequency of the VUV laser is held fixed on a given resonance to prepare a population in a selected Rydberg state. The millimetre waves are scanned and induce transitions from the selected Rydberg state to neighbouring Rydberg states. Because the bandwidth of the millimetre waves radiation is less than 1 kHz ( $3 \cdot 10^{-8} \text{ cm}^{-1}$ ) and the Doppler broadening in the wavenumber range  $4-6 \text{ cm}^{-1}$  is approximately 20 000 times less than at  $100\,000 \text{ cm}^{-1}$ , more than three orders of magnitude can be gained in the resolution. This gain in resolution is illustrated in Figure 3 which shows in the lower panel a millimetre waves spectrum of the transitions between the  $n = 62 d[3/2](J = 1)$  state of argon and  $p$  and  $f$  Rydberg states with  $n$  values in the range 68–71. Whereas the corresponding region of the VUV laser spectrum in Figure 2a appears spectrally congested because of the limited resolution, the millimetre waves spectrum consists of a series of perfectly resolved, sharp lines. The upper panel in Fig. 3 shows an expanded view of the transitions to the  $68f$  Rydberg states that appear as a doublet in the lower spectrum but are in fact a triplet of fine structure components split by the spin-orbit interaction [31].

At present our maximal resolution amounts to 60 kHz ( $2 \cdot 10^{-6} \text{ cm}^{-1}$ ) and is limited by the transit time of the molecules through the experimental region [32]. This resolution is amply sufficient to obtain the finest details of the energy level structure of high atomic and molecular Rydberg states. As an illustration, Figure 4a displays a millimetre waves spectrum of the transition between  $n = 51 d$  and  $55 p$  and  $f$  Rydberg states of  $H_2$  belonging to series converging to the  $N^+ = 1$  rotational level of the ortho- $H_2^+$  ion core. The upper spectrum in Fig. 4, recorded at a resolution of 1 MHz, shows an expanded view of the line marked by a vertical arrow in Fig. 4a and demonstrates that each line of the survey spectrum actually consists of several closely spaced lines. The Rydberg transition splits in a multitude of fine and hyperfine structure components and the millimetre waves spectrum contains the most detailed information that can be obtained on the complex interaction between the two nuclear spins  $I = 1/2$ , the molecular rotation  $N^+ = 1$ , the electron spin of the Rydberg electron  $s = 1/2$ , the electron spin of the ion core  $S^+ = 1/2$  and the electron orbital angular momentum  $l$  [33].

### 3. Electric Field Measurements Using High Rydberg States

Even weak electric fields profoundly alter the properties of high Rydberg states. Because the polarizability  $\alpha$  scales as  $n^7$  (see Table 1), the spectral position of low  $l$ , high  $n$  Rydberg states undergo appreciable quadratic Stark shifts  $\Delta\nu$  in the presence of an electric field of magnitude  $E$

$$\Delta\nu = 1/2\alpha E^2 \quad (2)$$

The weak and undefined stray electric fields that are inevitably present in most spectrometers and vacuum systems can easily falsify high-resolution spectroscopic measurements on high Rydberg states. These fields must be measured and compensated carefully. A convenient and very sensitive way of measuring these electric fields that we have developed for our studies [32] makes use of the large polarizability of the high Rydberg states themselves. The measurement procedure is illustrated in Fig. 5. A millimetre waves transition between two high Rydberg states (here between the  $n = 77 d[3/2](J = 1)$  and the  $91 f[5/2](J = 2)$  Rydberg states of the krypton atom) is recorded at high resolution as a function of the magnitude of an intentionally applied electric field. Because the spectral shift varies quadratically with the electric field strength, the line positions, when plotted as a function of the field strength, fall on a parabolic curve. At the apex of the parabola, the component of the electric field in the direction of the applied field has been exactly compensated, and the value of the applied compensation field corresponds to the negative value of the stray field (here  $-646 \pm 20 \mu\text{V}/\text{cm}$ ). The data in Fig. 5 show that stray fields weaker than  $1 \text{ mV}/\text{cm}$  can be measured in this way, and subsequently compensated with an accuracy of  $20 \mu\text{V}/\text{cm}$ .

This compensation procedure, however, only removes the spatially homogeneous component of the field and is not suited to eliminate electric field inhomogeneities. These inhomogeneities lead to an asymmetric inhomogeneous broadening of the spectral lines that becomes increasingly noticeable at increasing values of the electric field in Fig. 5. In our experiments, electric field inhomogeneities originate primarily from charged particles in the experimental volume that are inevitably produced by VUV laser radiation. Increasing the intensity of the VUV radiation leads to a marked increase in the inhomogeneous broadening. From the analysis of the broadened lineshapes, the inhomogeneous electric field distribution

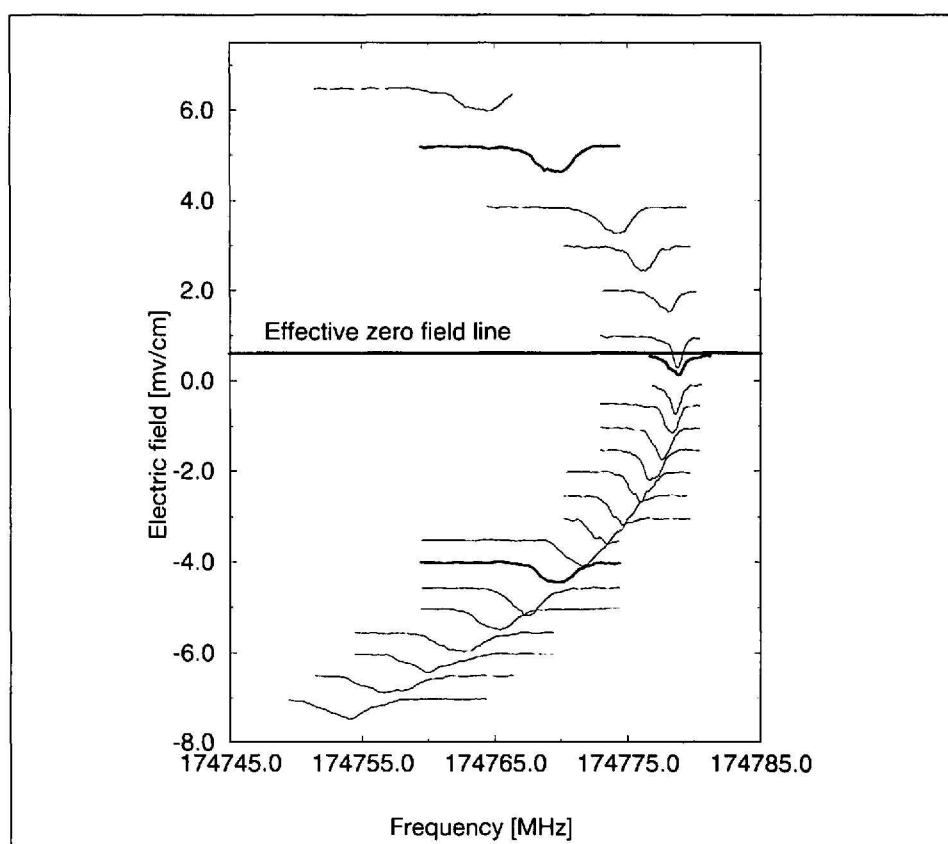


Fig. 5. Electric field measurements using high Rydberg states. The quadratic Stark shift of a transition between high Rydberg states (here the  $n = 77 d[3/2](J = 1)$  and the  $n = 91 f[5/2](J = 2)$  Rydberg states of krypton) is recorded as a function of the strength of an intentionally applied electric field (see text and Ref. [32] for additional details).

can be reconstructed and subsequently be used to precisely determine the ion concentration in the experimental volume (see Ref. [32] for more details).

Precise measurements of electric fields and ion concentrations such as those outlined here can be useful for a wide range of applications including the study of ion-molecule reactions, the investigation of plasmas and the determination of frequency standards.

### 4. Ion Spectroscopy Using High Rydberg States

Ions are difficult to study by high-resolution spectroscopy. The Coulomb repulsion forces between ions of the same charge and space-charge effects prevent the build up of concentrations much larger than  $ca. 10^{11} \text{ ions}/\text{cm}^3$  in the gas phase and cause significant Doppler broadening. Both effects reduce the applicability of high-resolution spectroscopic measurements to ions in the gas phase. Several important ions, such as  $\text{CH}_4^+$ , have so far remained completely impermeable to spectroscopic investigations.

The Rydberg spectrum offers a way to determine the energy level structure of

molecular ions. Indeed, Rydberg series exist that converge on every electronic, vibrational, rotational and hyperfine energy level of molecular ions. Detailed spectroscopic information on molecular ions can therefore be extracted from measurements of these series and subsequent extrapolation to the series limits. The advantages of this approach are a) that such measurements are carried out on neutral molecules and are not subject to the restrictions imposed by space-charged effects, and b) that the series limits can be determined at the same resolution as the Rydberg spectrum itself. The obvious disadvantage lies in the work that has to be invested in the analysis of the often very complex Rydberg spectra and in a correct extrapolation to  $n = \infty$ . Although we are currently developing and testing procedures [33] to extract precise spectroscopic information on molecular ions by comparing the extrapolated series limits determined from our high-resolution millimetre waves spectra of high Rydberg states of  $\text{H}_2$  (see above) with the well-known energy level structure of  $\text{H}_2^+$  [34], another experimental approach, pulsed-field-ionization zero-kinetic-energy (PFI-ZEKE) photoelectron spectroscopy [8][10–12] still is of greater practical significance.

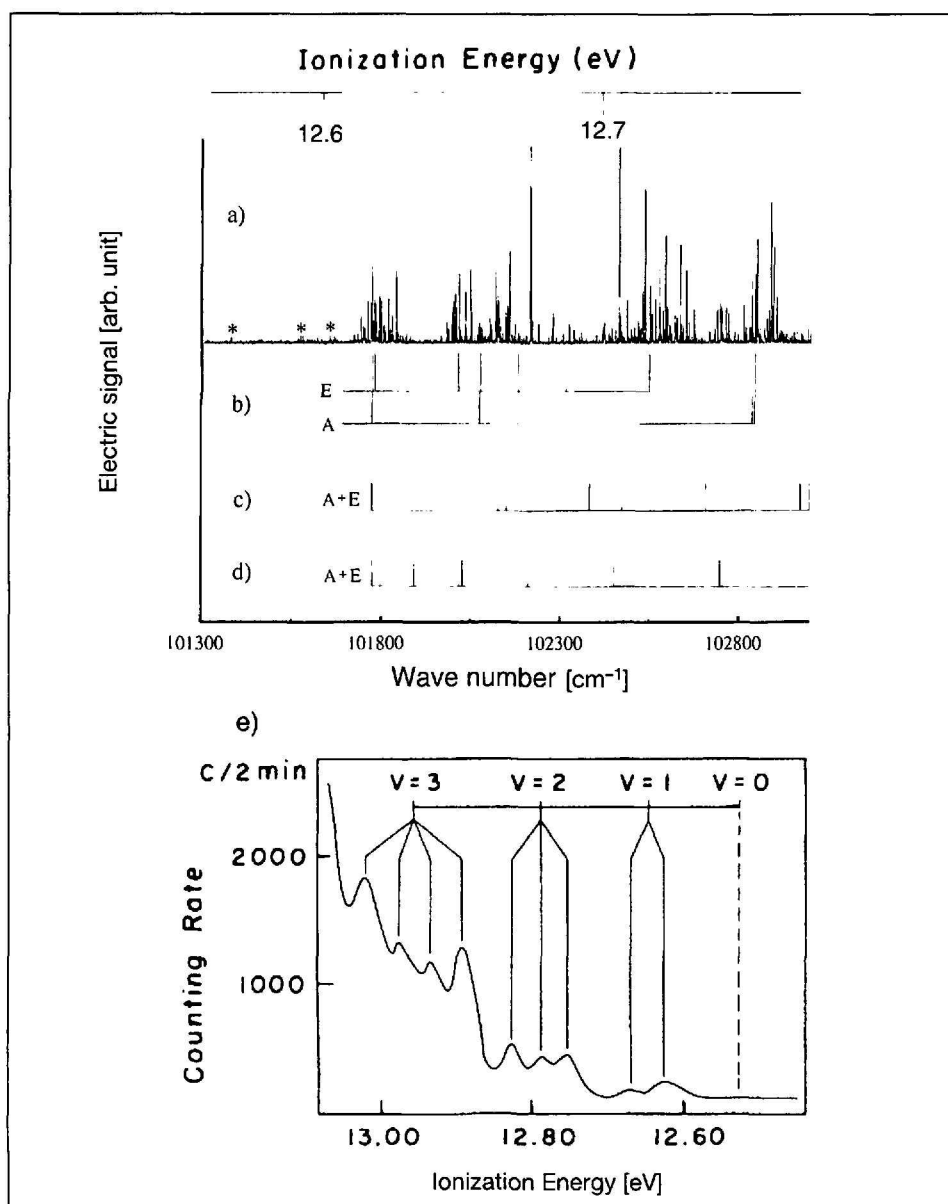


Fig. 6. Comparison of the HeI photoelectron spectrum of  $\text{CH}_4$  (lower trace, adapted from Ref. [50]) and the PFI-ZEKE photoelectron spectrum (upper panel, trace a). Traces b–d) in the upper panel indicate the results of model calculations of the vibrational structure based on various assumptions on the potential energy surface of the ground electronic state of  $\text{CH}_4^+$  (see Ref. [45] for additional details).

Table 2. The first adiabatic ionization potential of several molecules determined in our recent work by field ionization of high Rydberg states.

Molecule	Adiabatic ionization potential/ $\text{cm}^{-1}$	Reference
$\text{O}_2$	$97352.2 \pm 1.2$	[41]
$\text{Ar}_2$	$116591.1 \pm 6$	[49]
$\text{Kr}_2^a$	$103773.6 \pm 2$	[43]
$\text{H}_2\text{O}$	$101766.8 \pm 1.2$	[41]
$\text{CO}_2$	$111111.0 \pm 3$	[38]
OCS	$90195.4 \pm 5^b$	[39]
$\text{ND}_4$	$37490.7 \pm 1.5$	[44]
$\text{CH}_4$	$101773 \pm 35^c$	[45]
$\text{CDH}_3$	$101810.0 \pm 1.6$	[46]
$\text{CD}_2\text{H}_2$	$101852.3 \pm 1.4$	[47]
$\text{CD}_4$	$102197.1 \pm 1.5$	[46]

<sup>a</sup>Value determined for the  $^{84}\text{Kr}_2$  isotopomer. <sup>b</sup>Value obtained by subtracting the band centre of the  $\text{OCS}^+ \tilde{A}^2\Pi_{3/2}(000) \leftarrow \text{OCS}^+ \tilde{X}^2\Pi_{3/2}(000)$  transition measured by Ochsner *et al.*, [40] from the band centre of the  $\text{OCS}^+ \tilde{A}^2\Pi_{3/2}(000) \leftarrow \text{OCS}^+ \tilde{X}^1\Sigma(000)$  photoelectronic transition. <sup>c</sup>The uncertainty represents the half width at half maximum of the rotational contour of the lowest band in the photoelectron spectrum.

A PFI-ZEKE photoelectron spectrum is obtained by recording the pulsed field ionization of high Rydberg states (typically with  $n \geq 100$ ) as a function of the wavenumber of a tunable light source that is scanned through successive ionization thresholds. Because of the insufficient resolution of the laser sources used in PFI-ZEKE experiments, the individual Rydberg states that constitute a line in a PFI-ZEKE spectrum are not resolved. After a small correction (of typically less than  $8 \text{ cm}^{-1}$ ) is made to take into account the fact that these Rydberg states are actually located below the field-free ionization thresholds, each line in a PFI-ZEKE photoelectron spectrum can be interpreted as an energy difference between a level of an ion and one of its parent neutral molecule. The technique thus provides similar information as conventional HeI photoelectron spectroscopy, but at a considerably higher resolution.

Because the threshold field for field ionization decreases with increasing  $n$  values (see Table 1), the lines in a PFI-ZEKE photoelectron spectrum broaden towards lower frequencies at increasing pulsed ionization field strength. Moreover, the position and shape of the lines depend on the stray fields and the ion concentration in the experimental volume [35–37]. Consequently, a detailed characterization of stray fields and ion concentrations, for instance with the method presented in Section 3, turns out to be essential to optimize the sensitivity and the resolution of PFI-ZEKE photoelectron spectroscopic measurements, and to precisely calibrate the energy shift of the ionization thresholds induced by the pulsed electric fields. Two advantages result from a careful minimization of the stray fields: First, the highest Rydberg states can be observed by field ionization, and, second, very small pulsed electric fields can be used in the field ionization step. Both advantages help to improve the resolution and to detect only the highest Rydberg states, *i.e.* those that lie closest to the actual ionization limits. Ionization potentials can therefore be determined with improved accuracy. Table 2 lists accurate values for the lowest adiabatic ionization potential of several molecules determined in our recent studies.

At present, we can routinely record PFI-ZEKE photoelectron spectra at a resolution between  $0.2$  and  $0.3 \text{ cm}^{-1}$ . This resolution corresponds to the highest that has been achieved so far by photoelectron spectroscopy and has enabled us to obtain new spectroscopic information on the ground electronic states of several cations

such as  $O_2^+$  [41],  $Ar_2^+$  [42],  $Kr_2^+$  [43],  $OCS^+$  [39],  $H_2O^+$  [41],  $ND_4^+$  [44],  $CH_4^+$  [45],  $CDH_3^+$  [46],  $CD_2H_2^+$  [47],  $CD_4^+$  [46] and on several excited electronic states of  $O_2^+$  [48],  $N_2^+$  [25],  $Ar_2^+$  [49],  $OCS^+$  [39] and  $Kr_2^+$  [43]. It has also enabled us to characterize the structure of an intriguing, short-lived radical, the ammonium radical which, in its lowest metastable electronic state, is isoelectronic to the alkali metal atoms [44].

In the case of the methane cation, no rotationally resolved spectra had been obtained until the PFI-ZEKE photoelectron spectrum could be measured [45]. Fig. 6 compares the PFI-ZEKE photoelectron spectrum of  $CH_4^+$  (upper panel, trace a)) with the HeI photoelectron spectrum of Rabalais *et al.* [50] (lower panel). Thanks to the higher resolution, an extensive progression of sharp rotational lines can be observed in the PFI-ZEKE photoelectron spectrum whereas the HeI photoelectron spectrum only reveals a partially resolved vibrational structure. From the analysis of the complex vibrational and rotational structure of the PFI-ZEKE photoelectron spectrum, important structural and dynamical information have been extracted on  $CH_4^+$  [45] and its isotopomers  $CDH_3^+$  [46],  $CD_2H_2^+$  [47] and  $CD_4^+$  [46] which are all subject to a strong Jahn-Teller distortion in their electronic ground states.

## 5. Conclusions

The development of new light sources for VUV spectroscopy, and the combination of millimetre waves and VUV radiation in double-resonance experiments have greatly facilitated the experimental study of the spectroscopic and dynamical properties of high Rydberg states. The complete energy level structure of high Rydberg states, including the hyperfine structure, can be measured up to high values of the principal quantum number. High-resolution spectroscopy of high Rydberg states can also be used to carry out very precise measurements of stray electric fields and ion concentrations. Such measurements are essential to characterize and optimize the experimental conditions under which the spectra are recorded. Moreover, they greatly help to optimize the resolution that can be attained by photoelectron spectroscopy. At the current resolution limit of  $0.2\text{ cm}^{-1}$ , new information can be extracted by photoelectron spectroscopy on the energy level structure of important cations, and ionization potentials can be determined with high accuracy.

## Acknowledgements

I thank all my coworkers Dr. H. Palm, Dr. R. Signorell, Dr. B. Brupbacher-Gatehouse, Dr. M. Schäfer, A. Osterwalder, U. Hollenstein, A. Wüest, R. Seiler, H. Schmutz, R. Gunzinger, S. Willitsch, G. Petraglio and P. Rupper who have carried out an important part of the work described in this article. Our research is funded by the ETH Zürich and the Swiss National Science Foundation. Additional support was provided by the Robert Gnehm Stiftung.

Received: January 28, 2000

- [1] J.R. Rydberg, *K. svenska Vetensk. Akad. Handl.* **1889**, 23; J.R. Rydberg, *Z. Phys. Chem. (Leipzig)* **1890**, 5, 227.
- [2] G.D. Liveing, J. Dewar, *Proc. Roy. Soc. London* **1879**, 29, 398.
- [3] J.J. Balmer, *Pogg. Ann. d. Phys. u. Chem.* **1885**, 25, 80.
- [4] R.S. Mulliken, *J. Am. Chem. Soc.* **1964**, 86, 3183.
- [5] G.W. Series, in 'The Hydrogen Atom', Eds. G.F. Bassani, M. Inguscio, T.W. Hänsch, Springer, Berlin, **1989**, chapter 1, and references therein.
- [6] R.F. Stebbings, F.B. Dunning (Eds.), 'Rydberg States of Atoms and Molecules', Cambridge University Press, Cambridge, **1983**.
- [7] T.F. Gallagher, 'Rydberg Atoms', Cambridge University Press, Cambridge, **1994**.
- [8] G. Reiser, W. Habenicht, K. Müller-Dethlefs, E.W. Schlag, *Chem. Phys. Lett.* **1988**, 152, 119.
- [9] L. Zhu, P. Hohnson, *J. Chem. Phys.* **1991**, 94, 5769.
- [10] K. Müller-Dethlefs, E.W. Schlag, *Annu. Rev. Phys. Chem.* **1991**, 42, 109.
- [11] F. Merkt, T.P. Softley, *Int. Rev. Phys. Chem.* **1993**, 12, 205.
- [12] F. Merkt, *Ann. Rev. Phys. Chem.* **1997**, 48, 675.
- [13] M.S. Child (Ed.), 'Molecular Rydberg dynamics', Imperial College Press, London, **1999**.
- [14] C. Sándorfy (Ed.), 'The role of Rydberg states in spectroscopy and photochemistry', Kluwer Academic Publishers, Dordrecht, **1999**.
- [15] J.A.R. Samson, 'Techniques of vacuum ultraviolet spectroscopy', Pied Publications, Lincoln, **1967**.
- [16] J. Berkowitz, 'Photoabsorption, photoionization, and photoelectron spectroscopy', Academic Press, New York, **1979**.
- [17] P.A. Heimann, M. Koike, C.W. Hsu, D. Blank, X.M. Yang, A.G. Suits, Y.T. Lee, M. Evans, C.Y. Ng, C. Falim, H.A. Padmore, *Rev. Sci. Instrum.* **1997**, 68, 1945.
- [18] A.H. Kung, *Opt. Lett.* **1983**, 8, 24.
- [19] C.T. Rettner, E.E. Marinero, R.N. Zare, A.H. Kung, *J. Phys. Chem.* **1984**, 88, 4459.
- [20] R. Hilbig, G. Hilber, A. Lago, B. Wolff, R. Wallenstein, *Comments At. Mol. Phys.* **1986**, 18, 157.
- [21] T.P. Softley, W.E. Ernst, L.M. Tashiro, R.N. Zare, *Chem. Phys.* **1987**, 116, 299.
- [22] H.H. Fielding, T.P. Softley, F. Merkt, *Chem. Phys.* **1991**, 155, 257.
- [23] P. Levelt, W. Ubachs, *Chem. Phys.* **1992**, 163, 263.
- [24] J. W. Hepburn, in 'Laser Techniques in Chemistry', Eds. A.B. Myers, T.R. Rizzo, John Wiley and Sons, New York, **1995**.
- [25] H. Palm, F. Merkt, *Chem. Phys. Lett.* **1998**, 284, 419.
- [26] H. Palm, F. Merkt, *Appl. Phys. Lett.* **1998**, 73, 157.
- [27] F. Merkt, A. Osterwalder, R. Seiler, R. Signorell, H. Palm, H. Schmutz, R. Gunzinger, *J. Phys. B: At. Mol. Opt. Phys.* **1998**, 31, 1705.
- [28] U. Hollenstein, H. Palm, F. Merkt, in preparation.
- [29] H. Beutler, *Z. Physik* **1935**, 93, 177.
- [30] U. Fano, *Phys. Rev.* **1961**, 124, 1866.
- [31] F. Merkt, H. Schmutz, *J. Chem. Phys.* **1998**, 108, 10033.
- [32] A. Osterwalder, F. Merkt, *Phys. Rev. Lett.* **1999**, 82, 1831.
- [33] A. Osterwalder, R. Seiler, F. Merkt, in preparation.
- [34] K.B. Jefferts, *Phys. Rev. Lett.* **1969**, 23, 1476.
- [35] W.A. Chupka, *J. Chem. Phys.* **1993**, 98, 4520.
- [36] F. Merkt, *J. Chem. Phys.* **1994**, 100, 2623.
- [37] F. Merkt, R.N. Zare, *J. Chem. Phys.* **1994**, 101, 3495.
- [38] F. Merkt, S.R. Mackenzie, R.J. Rednall, T.P. Softley, *J. Chem. Phys.* **1993**, 99, 8430.
- [39] M. Sommovilla, F. Merkt, unpublished results.
- [40] M. Ochsner, M. Tsuji, J.P. Maier, *Chem. Phys. Lett.* **1985**, 115, 373.
- [41] F. Merkt, R. Signorell, H. Palm, A. Osterwalder, M. Sommovilla, *Mol. Phys.* **1998**, 95, 1045.
- [42] R. Signorell, A. Wüest, F. Merkt, *J. Chem. Phys.* **1997**, 107, 10819.
- [43] R. Signorell, U. Hollenstein, F. Merkt, in preparation.
- [44] R. Signorell, H. Palm, F. Merkt, *J. Chem. Phys.* **1997**, 106, 6523.
- [45] R. Signorell, F. Merkt, *J. Chem. Phys.* **1999**, 110, 2309.
- [46] R. Signorell, F. Merkt, submitted for publication.
- [47] R. Signorell, M. Sommovilla, F. Merkt, *Chem. Phys. Lett.* **1999**, 312, 139.
- [49] H. Palm and F. Merkt, *Phys. Rev. Lett.* **1998**, 81, 1385.
- [49] R. Signorell, F. Merkt, *J. Chem. Phys.* **1998**, 109, 9762.
- [50] J.W. Rabalais, T. Bergmark, L.O. Werme, L. Karlsson and K. Siegbahn, *Physica Scripta* **1971**, 3, 13.